Preprints of the 19th World Congress
The International Federation of Automatic Control
Cape Town, South Africa. August 24-29, 2014

# An LQG/LTR approach towards piezoactuator vibration reduction with observer-based hysteresis compensation ⋆

**Łukasz Ryba** * **Alina Voda** ** **Gildas Besançon** *,***

Control Systems Department
GIPSA-lab, BP 46, 38402 Saint-Martin d'Hères, France
Email: {lukasz.ryba, alina.voda,
gildas.besancon}@gipsa-lab.grenoble-inp.fr

* *Grenoble INP*
** *Joseph Fourier University - Grenoble 1*
*** *Institut Universitaire de France*

**Abstract:** This paper presents a SISO robust control of some lightly damped micro/nano-positioning system equipped with a piezoactuator. The adverse phenomenon of nonlinear hysteresis in the actuator is first compensated using an observer-based approach. Then an LQG/LTR method is proposed to additionally reduce vibrations affecting the system in a higher frequency range. Illustrative experimental results show a significant improvement of the closed-loop system behaviour with respect to the open-loop one.

*Keywords:* Micro/Nano-positioning, LQG/LTR, robust control, observer, hysteresis, vibration.

## 1. INTRODUCTION

Piezoelectric actuators, due to their high resolution, fairly high stiffness and fast response are commonly used in micro/nano-scale applications like in Scanning Tunneling Microscope (STM) or Atomic Force Microscope (AFM). On the other hand, they exhibit some adverse effects like hysteresis, mechanical vibration, creep or thermal noise. Nonlinear hysteresis can significantly reduce the accuracy especially in long-range positioning like during imaging large samples. When positioning over extended periods of time is required, the piezo can drift due to creep phenomenon, which also leads to the loss of precision. In imaging applications, one may want to achieve also high resolution of the scanned images, which takes sometimes several minutes or even fractions of an hour (Abramovitch et al., 2007). An increase of scanning frequency shortens that time but fast triangular waveforms may excite the resonance peaks of the positioning device and as a result the scanning speed is often limited to about 1% of piezo's first resonant frequency (Moheimani, 2008).

A large number of works has been devoted to overcoming those phenomena and they can be classified into open-loop and closed-loop methods. The open-loop feedforward control for both hysteresis and vibration can be found for example in Croft et al. (2001) (an inversion-based compensation), and in Rakotondrabe et al. (2010) (an inversion and input shaping compensation). The most popular models used for hysteresis, the Preisach (Hughes and Wen, 1997) and the Prandtl-Ishlinskii (PI) (Kuhnen and Janocha, 2001) models, though computationally intensive, are a common solution in cases where sensors are not available. On the other hand, closed-loop techniques are accurate and need not model inversion, but the drawback is that they require (sometimes expensive) sensors for feedback control. A simple proportional-integral (PI) controller often fails in dealing with highly resonant positioners. Popular feedback methods like Integral Resonant Controller (IRC) (Bhikkaji and Moheimani, 2008) or Positive Position Feedback controller (PPF) (Mahmood and Moheimani, 2009) can effectively surpress these vibration effects. One can also take advantage of known desired reference trajectory and use Repetitive Control (RC) as in Necipoglu et al. (2011). In Wu and Zou (2007) an iterative control approach (IIC) was used for compensating both, hysteresis and vibration of the piezo scanner during high-speed, large-range positioning. (Leang and S., 2002) combined high gain feedback (for hysteresis and creep) and feedforward inverse-based control (for vibration). Both bandwidth and scanning range can be increased significantly by using a dual actuated system (combination of long-range, low-bandwidth actuator with a short-range, high-bandwidth actuator) as Schitter et al. (2008a) or Kuiper et al. (2010) did for AFM. One can also increase AFM scanner's bandwidth by cutting a sharp top of the triangular reference trajectory (see Schitter et al. (2008b)).

In Yi et al. (2009), a disturbance observer (DOB) was proposed for hysteresis compensation. The idea is to consider hysteresis as a slowly varying disturbance on the input of a linear system, translate the difference between the response of the real plant and its model (through model inversion) into observed disturbance and substract it at the plant input. In the present paper, a similar DOB is implemented, with the difference that this

⋆ This work was partially supported by French ANR project CONFOC-AO.

 

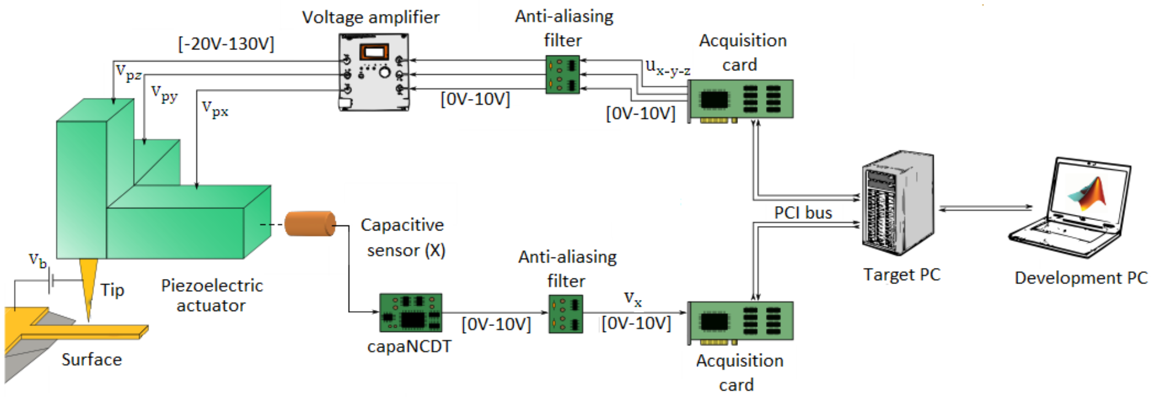


Fig. 1. Experimental setup.

disturbance is added as a new entry in a state vector of a simplified system (with one mode) and reconstructed via state observer (see Besançon et al. (2009)), which allows to compensate it directly witout model inversion.

In the recent years, a rapid growth of modern robust control designs has been recorded in mikro/nano-positioning due to uncertainties of different natures (different operating conditions, hysteresis, unmodelled dynamics etc.) (Sebastian and Salapaka, 2005). In Chuang et al. (2011) a robust $\mathcal{H}_\infty$ control for fast scanning in AFM in presence of sector bounded hysteresis uncertainty obtained much higher bandwidh than PID controller. Spatial resonant controller applied to piezoelectric laminate beam has been designed in order to minimize $\mathcal{H}_2$ norm of the system in Halim and Moheimani (2001). LQG control can be used as another damping technique as Habibullah et al. (2012) did for lateral positioning of an AFM. However, pure LQG controller is not guaranteed to be robust. It is commonly known that LQR controller (i.e. full state feedback quadratic optimal controller) has at least 60° phase margin, 6dB gain margin and thus provides always a stable closed loop system (Safonov and Athans (1977)). On the other hand, not all the states can be available either because there is a lack of sensors in the system or some states are simply impossible to measure. One can then incorporate a state observer to reconstruct the state of the system on the basis of the measured outputs (output feedback controller). However, the observer is based on the nominal model of the system, and its performance strongly depends on the level of system uncertainty. In this case the above mentioned robust stability margins of LQR solution are no more assured, since in practice the real plant differs from the nominal one and there is a need of robust controller which takes into account these differences. Moreover, even for minimum phase, open-loop stable systems, the margins can be arbitrairly small (Zhou et al. (1996), Doyle and Stein (1981)). In these cases, a simple approach of "speeding-up" observer dynamics of LQG design via properly chosen process and measurement covariance matrices may be not sufficient. To come out against lack of robustness of LQG, an LQG/LTR (Loop Transfer Recovery) procedure was proposed by Kwakernaak (1972), furtherly developped by Doyle and Stein (1979). Its main idea is to recover the desireable properties of LQR loop by relaxing the optimality either of the Kalman filter or quadratic feedback controller. This can be achieved by proper modification of their corresponding Algebric Riccatti Equations. This procedure can be done either w.r.t. the uncertainty on the plant intput or output and the system is assumed to be minimum phase.

In Munteanu and Ursu (2008), the application of LQG/LTR method is shown to successfully avoid dangerous vibration of the piezo smart composite wing of the aircraft. This technique has been also reported in Hu et al. (1999) and allowed to achieve high track density for dual-stage actuators in HDDs. In micro/nano-scale applications the LQG/LTR method was applied to piezoelectric tuning fork in AFM in vertical direction (Z-axis) (see Yeh et al. (2008)). However, as indicated in this work the hysteresis effect was omitted because of the small operating range (less than 100nm). This motivated us to check experimentally the efficiency of this method in terms of vibration reduction in the presence of nonlinear hysteresis of piezoactuator. The approach is applied to an STM-like mikro/nano-positioning platform under development in GIPSA-lab (Grenoble, France), in the horizontal fast scanning direction (X-axis), for which the induced vibration are unavoidable and play an important role for fast varying input voltages.

The paper is organized as follows: the experimental setup and system description are given in section 2. Section 3 is devoted to observer-based hysteresis compensation. Next, in Section 4 the identification and compensation of vibration is done using the LQG/LTR control procedure. Finally we conclude the paper in section 5.

## 2. EXPERIMENTAL SETUP AND SYSTEM DESCRIPTION

The considered experimental setup consists of a voltage amplifier E-240-100 (gain 15 [V/V] and bandwidth 4kHz), a piezoelectric actuator Tritor T-402-00 (gain 235 [nm/V] and bandwidth 630 Hz) and a capacitive sensor CS005 with capaNCDT 6500C measuring system (gain 200 [V/mm] and bandwidth 8.5 kHz) connected in cascade as shown in Fig. 1. The application designed in Matlab&Simulink$^{TM}$ and xPC Target$^{TM}$ software on development PC is downloaded via Ethernet interface into Target PC equipped with data acquisition card. The DAC forms an analog control signal 0-10 [V] which feeds the voltage amplifier. The ADC of the same board converts the output voltage 0-10 [V] from the capacitive sensor and returns the digital value to the real-time application running in Target PC. The sampling time is set to 20kHz.

This setup is designed as a tunneling current measurement system. In this paper we are focused only on the horizontal motion in X direction (a full 3-D problem formulation can be found in Ryba et al. (2013)). Both voltage amplifier and capacitive sensor can be described as first order systems (see Ryba et al. (2013)). On the other hand their bandwidths are relatively high (4kHz and 8.5 kHz, respectively) w.r.t. the bandwidth of the piezoactuator (630Hz) and the frequency of the signal to be tracked, thus they are assumed as constant gains ($G_{vx}$ and $G_{capx}$, respectively). In every notation we use subscript $x$ to indicate that we are focused on the X direction.

## 3. HYSTERESIS COMPENSATION

Two methods of hysteresis compensation were checked in our experiments. In the first approach, hysteresis is modelled using Prandtl-Ishlinskii (PI) model, while in the second approach a simple disturbance model is used in order to design a disturbance observer (DOB) for hysteresis reconstruction and compensation. It finally appeared that the second approach works better than the first one in terms of both simplicity and accuracy, as it is insensitive to model errors and in some way it adapts to changing conditions or to different initial settings of the capacitive sensor. In this paper only the second approach is presented for brevity. From now on, the time-dependence of variables will be omitted for simplicity.

A static nonlinear hysteresis $H_x[v_{px}]$ is considered here as:

$$H_x[v_{px}] = G_{px}(v_{px} + d_x(v_{px})) \tag{1}$$

where $d_x$ is a slowly varying disturbance acting on the input $v_{px}$ of the piezoactuator (see internal block in the whole scheme of Fig. 2).

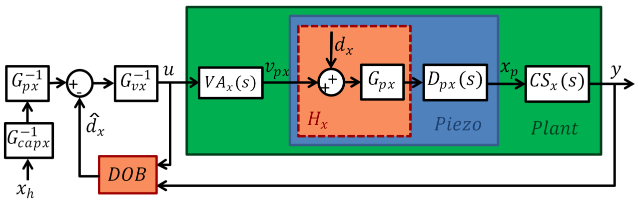


Fig. 2. Observer-based hysteresis compensation.

The following simplified second order model of the horizontal axis dynamics (including gain $G_{vx}$ of the input voltage amplifier $VA_x(s)$, piezo dynamics $D_x(s)$ and gain $G_{capx}$ of the capacitive sensor $CS_x(s)$) is used to get an estimation $\hat{d}_x$ of the low frequency disturbance $d_x$:

$$\begin{aligned}\ddot{x}_p + 2\xi_{px}\omega_{px}\dot{x}_p + \omega_{px}^2 x_p = \omega_{px}^2 \underbrace{G_{px}(v_{px} + d_x)}_{H_x[v_{px}]} = \\ \omega_{px}^2 \underbrace{(G_{px}G_{vx}u + G_{px}d_x)}_{H_x[u]} = \omega_{px}^2 G_{px}G_{vx}u + \omega_{px}^2 G_{px}d_x\end{aligned} \tag{2}$$

or in state-space (with state variables: $x_1 = x_p$, $x_2 = \dot{x}_p$):

$$\begin{aligned}\begin{pmatrix}\dot{x}_1\\ \dot{x}_2\end{pmatrix} &= \underbrace{\begin{pmatrix}0 & 1\\ -\omega_{px}^2 & -2\xi_{px}\omega_{px}\end{pmatrix}}_{A}\begin{pmatrix}x_1\\ x_2\end{pmatrix} \\ &+ \underbrace{\begin{pmatrix}0\\ \omega_{px}^2 G_{px}G_{vx}\end{pmatrix}}_{B} u + \underbrace{\begin{pmatrix}0\\ \omega_{px}^2 G_{px}\end{pmatrix}}_{B_d} d_x + w \\ y &= \underbrace{\begin{pmatrix}G_{capx} & 0\end{pmatrix}}_{C}\begin{pmatrix}x_1\\ x_2\end{pmatrix} + v\end{aligned} \tag{3}$$

where $u$ is the input voltage to the voltage amplifier $VA_x(s)$, $y$ is the output voltage from the capacitive sensor $CS_x(s)$, $w$ and $v$ are the process and measurement noises, respectively.

If the observer dynamics is sufficiently faster than the dynamics of disturbance $d_x$, the reconstruction is fast enough and the disturbance variations can be assumed constant ($\dot{d}_x \approx 0$) from the observer point of view.

Extending the state vector of (3) into $x_e = [x\ d_x]^T$ gives the following state space representation:

$$\begin{aligned}\dot{x}_e &= A_e x_e + B_e u + w\\ y &= C_e x_e + v\end{aligned} \tag{4}$$

where the matrices of an extended system are defined as

$$A_e = \begin{pmatrix}A & B_d\\ 0 & 0\end{pmatrix},\ B_e = \begin{pmatrix}B\\ 0\end{pmatrix},\ C_e = \begin{pmatrix}C & 0\end{pmatrix} \tag{5}$$

This system is checked to be observable, and its steady-state Kalman observer is given by:

$$\dot{\hat{x}}_e = A_e\hat{x}_e + B_e u + L(y - C_e\hat{x}_e) \tag{6}$$

where the observer gain matrix $L = PC_e^T V^{-1}$ can be chosen such that $\hat{x}_e$ is an optimal state estimate of (4) in terms of minimizing $E[\hat{x}_e - x_e]^T[\hat{x}_e - x_e]$ (the mean square error). $P$ is solution of Algebraic Riccati Equation (ARE):

$$A_e P + PA_e^T - LVL^T + W = 0 \tag{7}$$

Here, the covariance matrices $W$ and $V$ are chosen to guarantee proper dynamics of the observer taking into account both process and measurement noises.

Finally, the hysteretic dependency between the control input $u$ and the plant output $y$ can be obtained from the reconstructed disturbance $\hat{d}_x$ as follows:

$$y = \hat{H}_{xv}[u] = G_{capx}\hat{H}_x[u] = G_{capx}G_{px}(G_{vx}u + \hat{d}_x) \tag{8}$$

Fig. 3(a) shows a good consistency of the measured and reconstructed hysteresis between the input $u$ and output $y$. To compensate for the disturbance $d_x$, its estimate $\hat{d}_x$ is then substracted from the original piezo input voltage as shown in Fig. 2. In Fig. 3(b) the reference voltage $x_h$ (see Fig. 2) being a triangle of variable amplitude of 1, 3, 5 and 7V (which coresponds to the displacement $x_p$ of 5, 15 and 35 $\mu$m, respectively) and frequency 1 Hz was chosen and the corresponding output voltage $y$ was measured without (in red) and with (in blue) disturbance observer. The corresponding tracking performance is shown in Fig. 4(a), where it can be seen that the hysteresis is totally eliminated. Moreover, Fig. 4(b) shows that also creep phenomenon was successfully compensated. This cannot be achieved with PI model of hysteresis and it is another advantage of the present method. However,

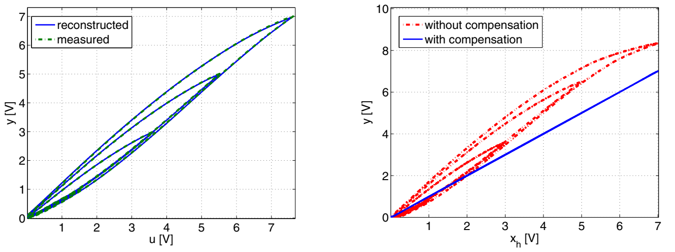


(a) (b)

Fig. 3. Hysteresis: (a) Reconstruction. (b) Compensation.

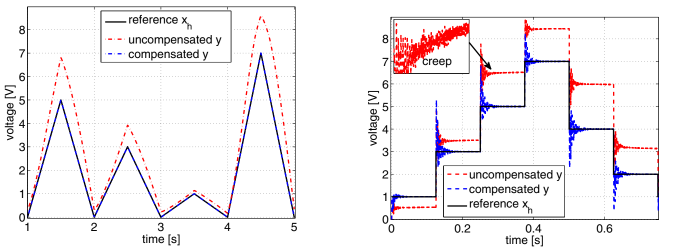


(a) (b)

Fig. 4. Reference tracking using observer-based approach: (a) Triangle of variable amplitude. (b) Steps.

the vibrations are still present and a method for their reduction will be presented in the next section.

## 4. VIBRATION COMPENSATION

In this section the vibration model is first identified, then its reduction is done using balanced truncation method and finally an LQG/LTR control is designed on the basis of this model.

### 4.1 Vibration model identification and model reduction

The model already compensated for hysteresis (see Fig. 2) with unit static gain, used as a vibration model, is identified here. The input identification signal $x_h$ is a chirp voltage of amplitude 0.5 V around 3 V with frequencies linearly growing with time from 0.1 Hz to Shannon frequency $0.5f_s$, where $f_s$ is the sampling frequency of 20 kHz. Fig. 5(a) shows the input/output identification data, and Fig. 5(b) the zoom of the model/measured data fitting near the first three resonant peaks (around 370, 620 and 1200 Hz). A continuous-time transfer function of order 16 is finally obtained, to catch a good vibration model.

However, this model is quite complex for control design, and a reduction is thus looked for. This is done here using balanced truncation method. First the full order model is converted to its balanced form and next the states which are weakly controllable/observable (with small corresponding singular values) are neglected. Fig. 6(a) depicts Hankel singular values of the full order model. The states with singular values less than 0.2 (on the right of the red line) are then neglected while keeping a minimum-phase behaviour and frequency responses of both full 16-order model and the resulting reduced 9-order model are shown in Fig. 6(b). One can notice good consistency between both models, despite order reduction.

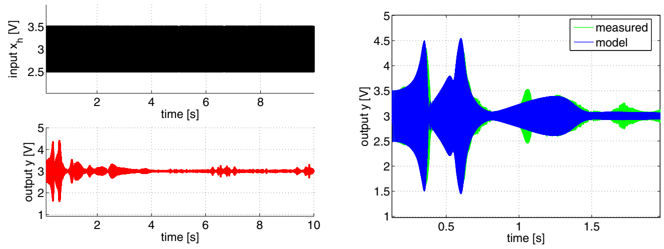


(a) (b)

Fig. 5. Model identification: (a) Input/output data. (b) Fitting the model into measured data.

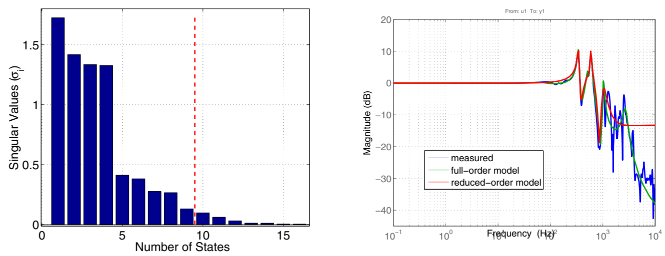


(a) (b)

Fig. 6. Model reduction: (a) Hankel singular values of full order model. (b) Frequency response of the real system, full and reduced order model.

### 4.2 Vibration reduction using LQG/LTR controller

On the basis of the obtained model, an LQG/LTR controller can be designed. This model is given by:

$$P_h : \begin{cases} \dot{x} = A_h x + B_h x_h + \xi; \quad x \in \mathbb{R}^9 \\ y = C_h x + \theta \end{cases} \tag{9}$$

where the substript $h$ means that the system is already compensated for hysteresis and $\xi$ and $\eta$ are its process and measurement noises, respectively.

The optimal LQR solution $x_h^* = -K_c x$ minimizes the following cost function on trajectories of (9):

$$J = \int_0^\infty (x^T Q x + x_h^T R x_h) dt \tag{10}$$

We consider here an LTR design on the plant output (it can be recovered also on the plant input, since the problems are dual). From Fig.7 one can see that the loop transfer function obtained by breaking the LQG loop at point $P_1$ ((Kalman Filter (KF) loop transfer function) is:

$$LTF_{P_1}(s) = C_h \Phi(s) K_f; \quad \Phi(s) = (sI_{9\times 9} - A_h)^{-1} \tag{11}$$

and the loop transfer function obtained by breaking the LQG loop at point $P_2$ is:

$$LTF_{P_2}(s) = P_h(s) K_{LQG/LTR}(s) \tag{12}$$

Now, the aim of LTR procedure is to make $LTF_{P_2}(s)$ to approach to $LTF_{P_1}(s)$ by properly designed LQR controller. In other words, the LQG/LTR design consists of two steps:
1) Loop transfer design - design LQG loop transfer function on the basis of LQR (full-state feedback) at point $P_1$.
2) Loop transfer recovery (LTR) - approximate the desired

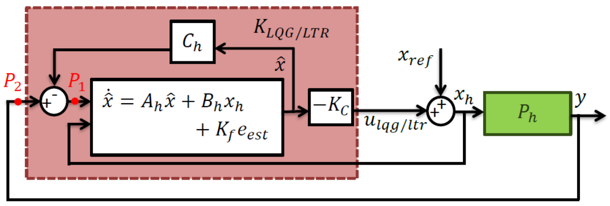


Fig. 7. LQG/LTR feedback loop.

loop transfer function obtained from step 1 with a recovery procedure at point $P_2$ (plant output).

*Step 1):* (the full state design) is done via KF ARE:

$$A_h P + P A_h^T - K_f \Theta K_f^T + \Xi = 0 \quad (13)$$

where $\Xi = E[\xi\xi^T] = B_h B_h^T$, $\Theta = E[\theta\theta^T] = \rho I_{1\times 1}$, $\rho = 1$ are the process and measurement covariance matrices.

*Step 2):* (LQR loop recovery at plant output) is done via LQR ARE:

$$A_h^T S + S A_h - K_c^T R K_c + Q = 0 \quad (14)$$

where $Q = qC_h^T C_h$, $R = I_{1\times 1}$ are the weighting matrices for state and control effort in (10).

The Nyquist plots of the recovered loop transfer function are depicted in Fig.8. One can observe the convergence to the desired optimal LQR loop transfer function when increasing recovery gain $q$. The obtained state-space LQG/LTR controller, based on the reduced nominal model is applied to the real plant, already compensated for hysteresis (see Fig.9). Fig.10 shows the chirp response in open-loop (red) and in closed-loop (blue). One can see that with this controller the vibrations are reduced near the resonant peaks w.r.t. the open-loop response.

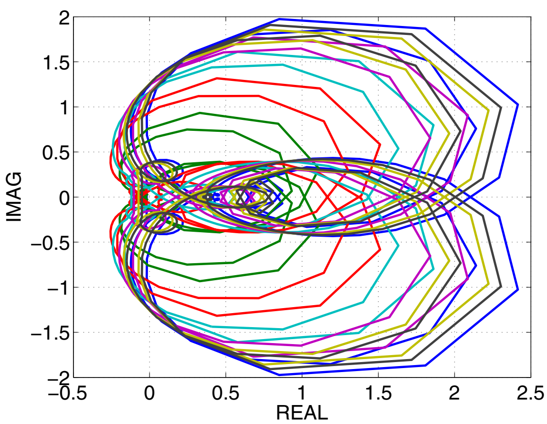


Fig. 8. Nyquist plots of $LTF_{P_2}(s)$ with increasing recovery gain $q = [1, 10, 10^2, 10^3, 10^4, 10^5, 10^6]$ (from green to black, respectively. The desired $LTF_{P1}(s)$ is in blue).

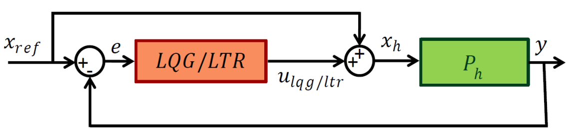


Fig. 9. LQG/LTR control.

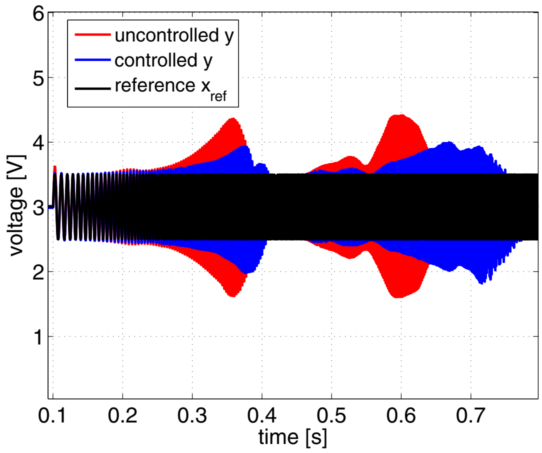


Fig. 10. System response for chirp signal.

The final results for tracking triangular reference trajectories of 100, 200 and 300 Hz respectively are presented in Fig.11. First the system is uncontrolled and at some time (red line in Fig.11) the LQG/LTR controller is switched on. One can see vibration reduction in all cases w.r.t. the open-loop behaviour, especially for higher frequency cases.

## 5. CONCLUSION

In this paper a robust LQG/LTR control for vibration reduction was implemented and tested in experiments for one axis of a mikro/nano-positioning system. Nonlinear hysteresis was beforehand compensated using observer-based approach. The experimental results show a significant improvement of the controlled system w.r.t. the uncontrolled one. It has to be stressed out that further improvement of tracking could be obtained for example by inclusion frequency dependent weighting matrices into quadratic cost function, instead of the static ones.

## REFERENCES

Abramovitch, D., Andersson, S., Pao, L.Y., and Schitter, G. (2007). A tutorial on the mechanisms, dynamics, and control of atomic force microscopes. In *American Control Conf., 2007*, 3488–3502.

Besançon, G., Voda, A., and Jourdan, G. (2009). Kalman observer approach towards force reconstruction from experimental afm measurements. In *15th IFAC Symp. on System Identification*, 1381–1386.

Bhikkaji, B. and Moheimani, S.O.R. (2008). Integral resonant control of a piezoelectric tube actuator for fast nanoscale positioning. *IEEE/ASME Trans. on Mechatronics*, 13(5), 530–537.

Chuang, N., Petersen, I., and Pota, H. (2011). Robust $\mathcal{H}_\infty$ control in fast atomic force microscopy. In *American Control Conf., 2011*, 2258–2265.

Croft, D., Shed, G., and Devasia, S. (2001). Creep, hysteresis, and vibration compensation for piezoactuators: Atomic force microscopy application. *J. of Dynamic Systems, Measurement, and Control*, 123(1), 35–43.

Doyle, J.C. and Stein, G. (1979). Robustness with observers. *IEEE Trans. on Auto. Control*, 607–611.

Doyle, J.C. and Stein, G. (1981). Multivariable feedback design: Concepts for a classical/modern synthesis. *IEEE Trans. on Auto. Control*, 4–16.

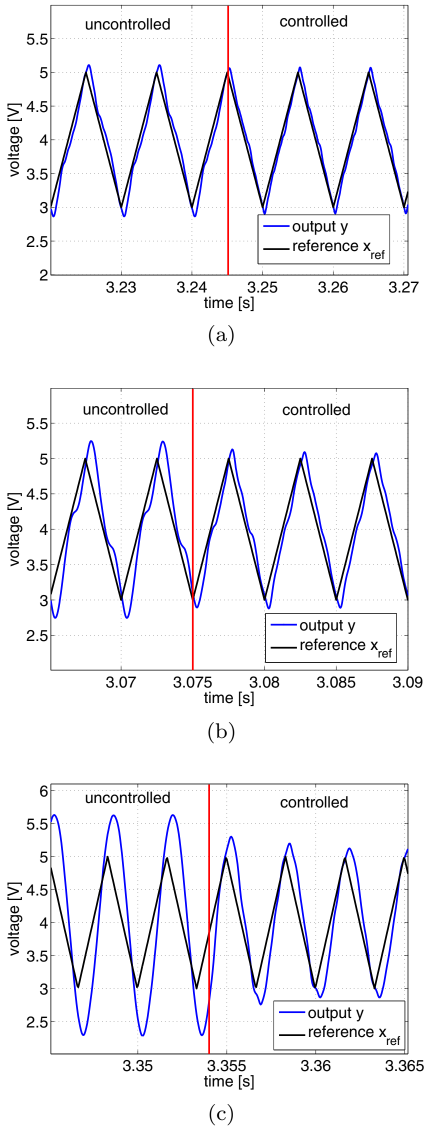


Fig. 11. Reference tracking: (a) 100, (b) 200, (c) 300 Hz.

Habibullah, H., Rehman, O., Pota, H., and Petersen, I. (2012). Internal reference model based optimal lqg controller for atomic force microscope. In *12th Intern. Conf. on Control Automation Robotics Vision (ICARCV 2012)*, 294–299.

Halim, D. and Moheimani, S.O.R. (2001). Spatial resonant control of flexible structures-application to a piezoelectric laminate beam. *IEEE Trans. on Control Systems Technology*, 9(1), 37–53.

Hu, X., Guo, W., Huang, T., and Chen, B. (1999). Discrete-time lqg/ltr dual-stage controller design and implementation for high track density hdds. In *Proceedings of the 1999 American Control Conf.*, volume 6, 4111–4115.

Hughes, D. and Wen, J. (1997). Preisach modeling of piezoceramic and shape memory alloy hysteresis. *Smart Materials and Structures*, 6(3), 287.

Kuhnen, K. and Janocha, H. (2001). Inverse feedforward controller for complex hysteretic nonlinearities in smart-material systems. *Control of Intell. Syst.*, 29(3), 74–83.

Kuiper, S., Fleming, A., and Schitter, G. (2010). Dual actuation for high speed atomic force microscopy. In *5th IFAC Symp. on Mechatronic Systems*, 220–226.

Kwakernaak, H. (1972). *Linear Optimal Control Systems.* John Wiley & Sons, Inc., New York, NY, USA.

Leang, K. and S., D. (2002). Iterative control approach to compensate for the hysteresis and the vibrational dynamics effects of piezo actuators. In *IFAC Conf.Mech.Syst., 2002*, 283–289.

Mahmood, I. and Moheimani, S.O.R. (2009). Improvement of accuracy and speed of a commercial afm using positive position feedback control. In *American Control Conf., 2009*, 973–978.

Moheimani, S.O.R. (2008). Accurate and fast nanopositioning with piezoelectric tube scanners: Emerging trends and future challenges. *Rev. Sci. Instrum.*, 79(7), 071101–071101–11.

Munteanu, E. and Ursu, l. (2008). Piezo smart composite wing with lqg/ltr control. In *IEEE Intern. Symp. on Industrial Electronics, (ISIE 2008)*, 1160–1165.

Necipoglu, S., Cebeci, S., Basdogan, C., Has, Y., and Guvenc, L. (2011). Repetitive control of an xyz piezo-stage for faster nano-scanning: Numerical simulations and experiments. *Mechatronics*, 21(6), 1098 – 1107.

Rakotondrabe, M., Clevy, C., and Lutz, P. (2010). Complete open loop control of hysteretic, creeped, and oscillating piezoelectric cantilevers. *IEEE Trans. on Automation Science and Engineering*, 7(3), 440–450.

Ryba, L., Voda, A., and Besançon, G. (2013). Modelling and control of 3d stm-like scanning device with application to surface reconstruction. In *Proceedings of the 2013 18th Intern. Conf. on Methods and Models in Automation and Robotics (MMAR 2013)*, 479–484.

Safonov, M. and Athans, M. (1977). Gain and phase margin for multiloop lqg regulators. *IEEE Trans. on Automatic Control*, 22(2), 173–179.

Schitter, G., Rijkee, W., and Phan, N. (2008a). Dual actuation for high-bandwidth nanopositioning. In *47th IEEE Conf. on Decision and Control, 2008*, 5176–5181.

Schitter, G., Thurner, P.J., and Hansma, P.K. (2008b). Design and input-shaping control of a novel scanner for high-speed atomic force microscopy. *Mechatronics*, 18(56), 282 – 288.

Sebastian, A. and Salapaka, S. (2005). Design methodologies for robust nano-positioning. *IEEE Trans. on Control Systems Technology*, 13(6), 868–876.

Wu, Y. and Zou, Q. (2007). Iterative control approach to compensate for both the hysteresis and the dynamics effects of piezo actuators. *IEEE Trans. on Control Systems Technology*, 15(5), 936–944.

Yeh, T.J., Wang, C.D., and Wu, T.Y. (2008). Modeling and control of an atomic force microscope using a piezoelectric tuning fork for force sensing. *Simulation Modelling Practice and Theory*, 16(7), 768–782.

Yi, J., Chang, S., and Shen, Y. (2009). Disturbance-observer-based hysteresis compensation for piezoelectric actuators. *IEEE/ASME Trans. on Mechatronics*, 14(4), 456–464.

Zhou, K., Doyle, J.C., and Glover, K. (1996). *Robust and optimal control.* Prentice-Hall, Inc., Upper Saddle River, NJ, USA.